

# Assembly of imino nitroxides with Ag(I) and Cu(I) ions

Hiroki Oshio \*, Tasuku Ito

*Department of Chemistry, Graduate School of Science, Tohoku University, Sendai 980-8578, Japan*

Received 1 April 1999; received in revised form 9 September 1999; accepted 4 November 1999

## Contents

Abstract . . . . .	329
1. Introduction . . . . .	330
2. Experimental . . . . .	330
3. Magnetic interactions between radical centres through diamagnetic metal ions . . . . .	330
3.1 [Cu(I)(imme <sub>2</sub> py) <sub>2</sub> ](PF <sub>6</sub> ) . . . . .	331
3.2 Ag(I)(impy) <sub>2</sub> (PF <sub>6</sub> ) . . . . .	332
3.3 Propagation of the ferromagnetic interaction in [Cu(I)(imme <sub>2</sub> py) <sub>2</sub> ](PF <sub>6</sub> ) and [Ag(I)-(impy) <sub>2</sub> ](PF <sub>6</sub> ) . . . . .	333
4. Assemblies with Cu(I) halides . . . . .	335
4.1 Two-dimensional network of imino nitroxides in [Cu(μ-I)(impy)] <sub>2</sub> and [Cu(μ-I)-(imme <sub>2</sub> py)] <sub>2</sub> . . . . .	336
4.2 Radical cubane of [Cu <sub>4</sub> Br <sub>4</sub> (bisimph) <sub>2</sub> ] . . . . .	338
5. Radical helix of Cu(II) imino nitroxide . . . . .	339
6. Helical assembly of imino nitroxide diradical with Ag(I) ions . . . . .	340
7. Conclusion . . . . .	344
Acknowledgements . . . . .	344
References . . . . .	345

## Abstract

Magnetic interactions between coordinated imino nitroxides through the diamagnetic Cu(I) and Ag(I) ions, and radical assemblies by means of coordination to Ag(I) and Cu(I) ions are discussed. © 2000 Elsevier Science S.A. All rights reserved.

**Keywords:** Radical helix; Supramolecule; Copper; Silver; Imino nitroxide; Magnetism

\* Corresponding author. Fax: +81-22-2176548.

E-mail address: oshio@agnus.chem.tohoku.ac.jp (H. Oshio)

## 1. Introduction

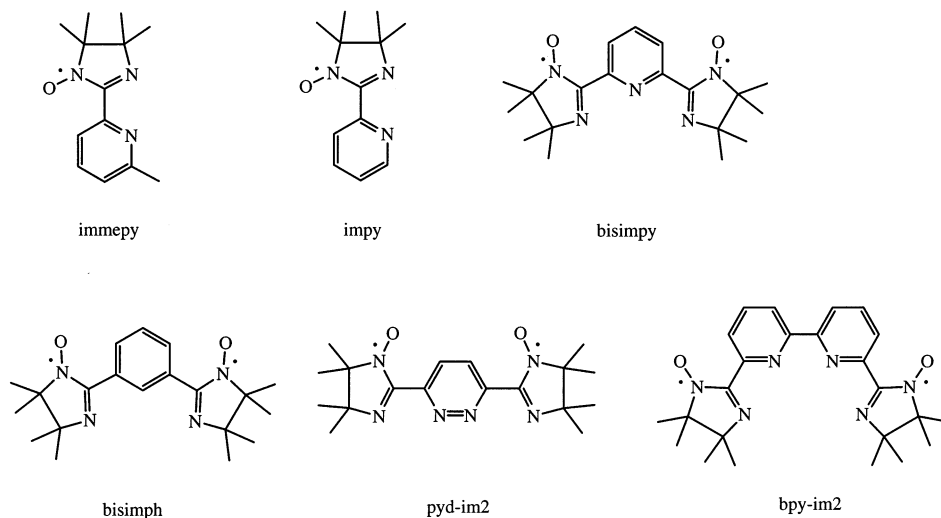
Supramolecular chemistry of coordination compounds is the subject of intense research interest [1–4]. It has been known for several years that the self-assembly of oligopyridyl strands with Ag(I) and Cu(I) ions give well organized molecular architectures such as inorganic grids [5], double-[6–8], and triple-[9,10] stranded metal helicates. A general feature of such diamagnetic metal ions as a component of the self-assembled system is that the tetrahedral coordination algorithm can give a helicate formation to the oligopyridyl strands. If organic radicals are introduced into such oligopyridyl strands, the radicals are self-assembled to form radical-supramolecules. The radical assembly by means of a metal ion may also provide an opportunity to synthesize novel organic magnetic materials such as helical and chiral magnets. Such molecular based chiral magnets might be used to study a relationship between natural optical activity and magnetic field induced circular dichroism, which is the so-called magneto-chiral dichroism proposed in 1984 [11] and experimentally confirmed for the molecular compound in 1997 [12]. On the other hand, Cu(I) halocuprates exhibit a wide variety of structures and molecules form discrete geometry of varying nuclearity or polymeric extended systems [13–20]. The introduction of organic radicals into the halocuprate cluster or network may also provide an opportunity to design an interesting magnetic material. In this paper, we review the magnetic interactions between radical centers through diamagnetic metal ions and radical assemblies by means of direct coordination to diamagnetic metal ions and to halocuprates.

## 2. Experimental

Mono- and di-imino nitroxides were prepared from each formyl derivative using the Ulman method [21]. The ligands in this review and their abbreviations are shown in Scheme 1.

## 3. Magnetic interactions between radical centers through diamagnetic metal ions

Typically, magnetic interactions between paramagnetic centers through diamagnetic metal ions are negligibly small or weakly antiferromagnetic. Trinuclear systems such as dimethylglyoximate-bridged Cu(II)–Ni(II)(LS)–Cu(II) [22] and Fe(III)–Fe(II)(LS)–Fe(III) (LS = low-spin) [23] complexes showed weak antiferromagnetic interactions ( $J = -2.6$  and  $-4.4 \text{ cm}^{-1}$ , respectively) between the terminal metal ions. However, a moderately strong antiferromagnetic interaction ( $J = -36 \text{ cm}^{-1}$ ) has been observed for an analogous Cu(II)–Pd(II)–Cu(II) complex [20]. Diamagnetic metal complexes with semiquinones also show a variety of magnetic interactions depending on the metal ions and coordination geometries. A series of square planar metal complexes  $[\text{M}(\text{SQ})_2]$  ( $\text{M} = \text{Ni(II)}, \text{Pd(II)}, \text{and Pt(II)}$ ) ( $\text{SQ} = \text{tert-butyl-substituted semiquinone}$ ) show fairly strong antiferromagnetic in-



Scheme 1.

interactions due to indirect overlap of the magnetic orbitals through the metal  $d\pi$  orbitals [24,25]. The strength of the inter-radical exchange increases down the series of metal ions; i.e. the strongest coupling for Pt and the weakest for Ni. On the other hand, pseudo-octahedral coordination geometry provides orthogonal coordination of semiquinones.  $[M(III)(3,6\text{-DBSQ})_3]$  ( $M = \text{Al}$  and  $\text{Ga}$ , and  $3,6\text{-DBSQ} = 3,6\text{-di-}t\text{-tert-butylsemiquinone}$ ) [26] and  $[\text{Ga(III)}(3,5\text{-dtbsq})_3]$  ( $3,5\text{-dtbsq} = 3,5\text{-di-}t\text{-tert-butyl-1,2-benzosemiquinone}$ ) [27,28] showed weak ferromagnetic interactions ( $J = 6.2, 8.6,$  and  $7.8 \text{ cm}^{-1}$  where  $H = -2J \sum S_i \cdot S_j$ ), while  $[M(IV)(\text{Cat-N-SQ})_2]$  ( $M = \text{Ti}, \text{Ge},$  and  $\text{Sn}$ ) ( $\text{Cat-N-SQ} = \text{tridentate Schiff base biquinone}$ ) [29] were characterized by a triplet ground state with exchange coupling constants of  $J = -56, -27,$  and  $-23 \text{ cm}^{-1}$  ( $H = J \sum S_1 \cdot S_2$ ), respectively. The magnitude of these magnetic interactions through diamagnetic ions depends strongly on the energy of the  $d$  orbitals. Here we discuss magnetic interactions between imino nitroxides through diamagnetic  $\text{Cu(I)}$  and  $\text{Ag(I)}$  ions [30,31].

### 3.1. $[\text{Cu(I)}(\text{immepy})_2](\text{PF}_6)$

In  $[\text{Cu(I)}(\text{immepy})_2](\text{PF}_6)$  (Fig. 1), the  $\text{Cu(I)}$  ion has two coordinated immepy acting as bi-dentate ligands. The coordination geometry about the  $\text{Cu}$  ion is pseudotetrahedral with the four coordination sites of the  $\text{Cu}$  ion being occupied by four nitrogen atoms. The  $\text{Cu-N}(\text{imino nitroxide})$  bond is slightly shorter ( $1.953(5) \text{ \AA}$ ) than the  $\text{Cu-N}(\text{pyridine})$  bond ( $2.081(6) \text{ \AA}$ ). The two coordination planes, and hence the two radical moieties characterized as  $\text{O-N-C-N}$  planes (magnetic orbitals) are perpendicular to each other with a dihedral angle of  $88.7^\circ$ .

The magnetic susceptibility data revealed that the ferromagnetic interaction between the coordinated imino nitroxides was operative through the Cu(I) ion and the exchange interaction  $J$  ( $H = -JS_1 \cdot S_2$ ) was estimated to be  $55.1(6) \text{ cm}^{-1}$ . The observed ferromagnetic interaction is due to the orthogonal arrangement of the coordinated imino nitroxides. The  $[\text{Cu(I)(immepy)}_2](\text{PF}_6)$  showed a strong absorption band at 766 nm which can be assigned to the MLCT band (from  $e(d_{xz}, d_{yz})$  orbital to the radical SOMO). The  $\pi$ -back donation, which mixes the  $e(d_{xz}, d_{yz})$  orbital and SOMO, induces a large spin delocalization of the coordinated radical SOMOs onto the Cu(I) ion; the resultant spin on the degenerate  $d\pi$  orbitals ( $d_{xz}, d_{yz}$ ) of Cu(I) ion leads to the strong ferromagnetic interaction.

### 3.2. $\text{Ag(I)(impy)}_2(\text{PF}_6)$

The Ag(I) ion in  $[\text{Ag(I)(impy)}_2](\text{PF}_6)$  (Fig. 2) has a distorted tetrahedral coordination environment with two coordinated imino nitroxides, where the dihedral angle between the radical planes deviates from the orthogonal ( $79.2^\circ$ ). The average bond lengths between the Ag(I) ion and the coordinated nitrogen atoms are 2.375 and 2.228 Å for Ag–N(pyridine) and Ag–N(imino nitroxide), respectively.

Temperature dependent epr measurements of the acetonitrile solution, where a solution experiment excludes the possibility of an intermolecular magnetic interaction, revealed that the Curie plot of the signal intensity for the  $\Delta m = 2$  transition gave positive  $\theta$  value of 4 K. This means the amplitude of the ferromagnetic intramolecular interaction in  $[\text{Ag(I)(impy)}_2](\text{PF}_6)$  is very small. The fairly weak ferromagnetic interaction in the Ag(I) complex compared with Cu(I) complex is due to the broken orthogonality and the lack of the MLCT interaction discussed in the next section.

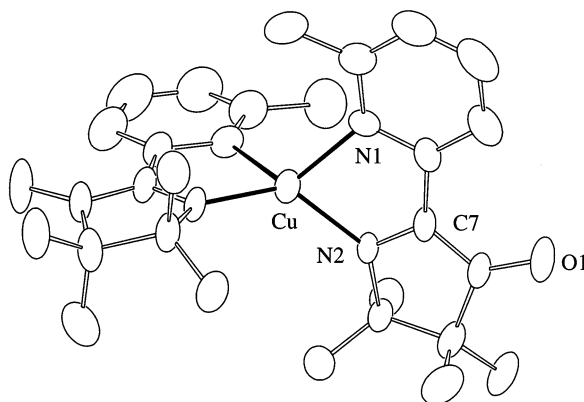


Fig. 1. The structure of  $[\text{Cu(I)(immepy)}_2]^+$ .

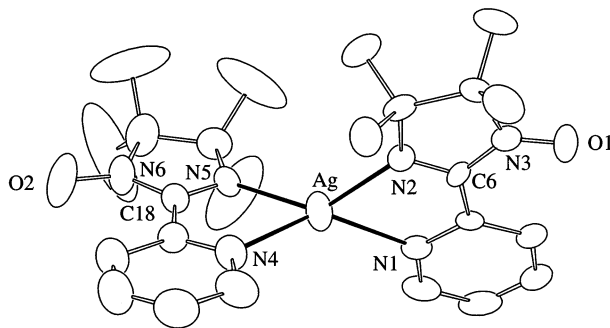


Fig. 2. The structure of  $[\text{Ag}(\text{I})(\text{impy})_2]^+$ .

### 3.3. Propagation of the ferromagnetic intercation in $[\text{Cu}(\text{I})(\text{impepy})_2](\text{PF}_6)$ and $[\text{Ag}(\text{I})(\text{impy})_2](\text{PF}_6)$

$[\text{Cu}(\text{I})(\text{impepy})_2](\text{PF}_6)$  shows a fairly strong ferromagnetic interaction, while the ferromagnetic interaction in  $[\text{Ag}(\text{I})(\text{impy})_2](\text{PF}_6)$  is very weak. UV–vis spectra for the complexes may give some insight to interpret this magnetic property of the radical dimer. The UV–vis absorption spectra of the two complexes along with the impepy ligand shows interesting features (Fig. 3).

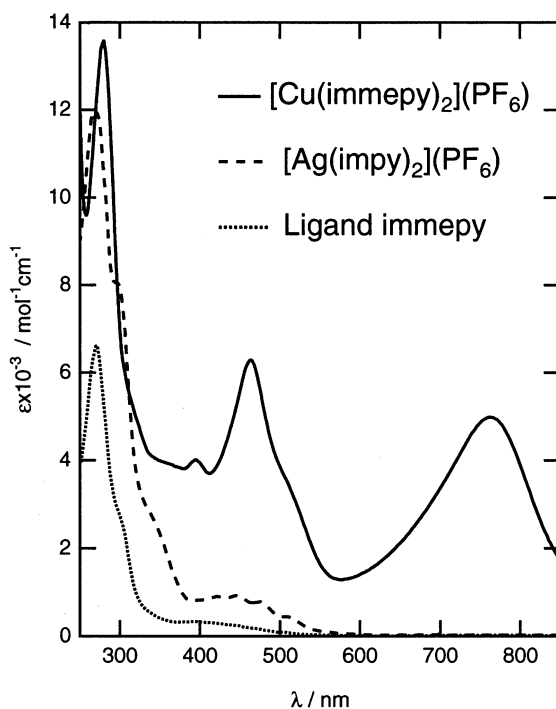
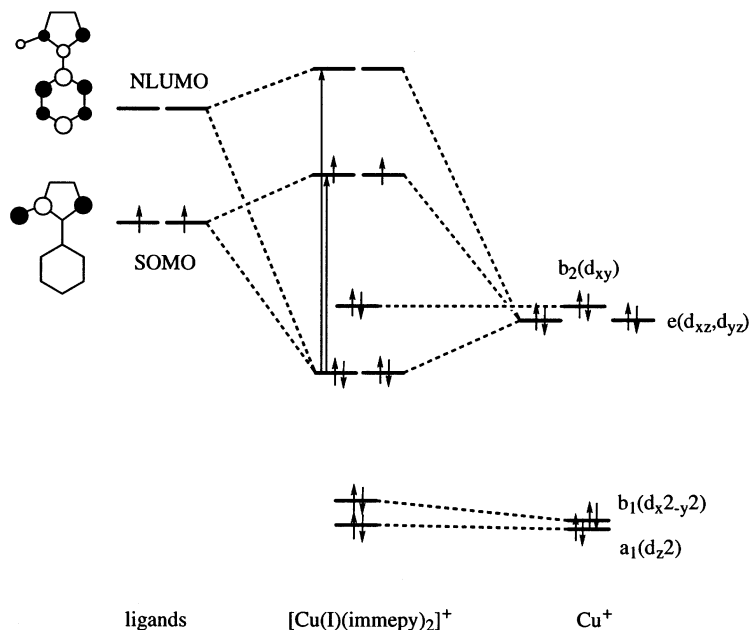


Fig. 3. The UV–vis spectra of  $[\text{Cu}(\text{I})(\text{impepy})_2](\text{PF}_6)$ ,  $[\text{Ag}(\text{I})(\text{impy})_2](\text{PF}_6)$ , and ligand impepy in acetonitrile.

In acetonitrile solution,  $[\text{Cu(I)(impepy)}_2](\text{PF}_6)$  shows intense absorption bands at 766 nm ( $\varepsilon = 5000 \text{ M}^{-1} \text{ cm}^{-1}$ ) and 464 nm ( $\varepsilon = 6300 \text{ M}^{-1} \text{ cm}^{-1}$ ) with a shoulder band at 510 nm. A PM3 molecular orbital calculation for the ligand impepy (where the iminonitroxide fragment and the pyridine ring are coplanar) shows that the singly occupied molecular orbital (SOMO) is centered mainly on the iminonitroxide fragment, while the next lowest unoccupied orbital (NLUMO) is delocalized over the whole  $\pi$  system. Both the SOMO and the NLUMO are of proper symmetry to overlap with the  $d_{xz}$  and  $d_{yz}$  orbitals of the copper ion. The lower energy band (766 nm) can therefore be assigned to an  $e(d_{xz}, d_{yz})$  to SOMO transition and the shoulder at 510 nm to  $b_2(d_{xy})$  to NLUMO, while the higher energy band (464 nm) is assigned to  $e(d_{xz}, d_{yz})$  to NLUMO (Scheme 2).

The strong ferromagnetic interaction can be attributed to the charge transfer interaction, a strong absorption band at 764 nm which corresponds to electron transfer from the  $e(d_{xz}, d_{yz})$  orbital to the SOMO (radical). The  $\pi$ -back donation, which mixes the  $e(d_{xz}, d_{yz})$  orbital and SOMO, induces a large spin delocalization of each coordinated iminonitroxide onto the Cu(I) ion; the resultant spin on the Cu(I) ion result in the strong ferromagnetic interactions. On the other hand,  $[\text{Ag(I)(impy)}_2](\text{PF}_6)$  does not show any metal to ligand charge transfer bands in UV–vis region (Fig. 3). Therefore, there is an apparent energy mismatch between the ligand  $\pi^*$  and  $d\pi$  orbital of the Ag(I) ion. Thus not only the broken orthogonality, but also the lack of the charge transfer interaction between the Ag(I) ion and iminonitroxides stabilizing the high-spin state, make the intramolecular ferromagnetic interaction very weak in the case of  $[\text{Ag(I)(impy)}_2](\text{PF}_6)$ .



Scheme 2.

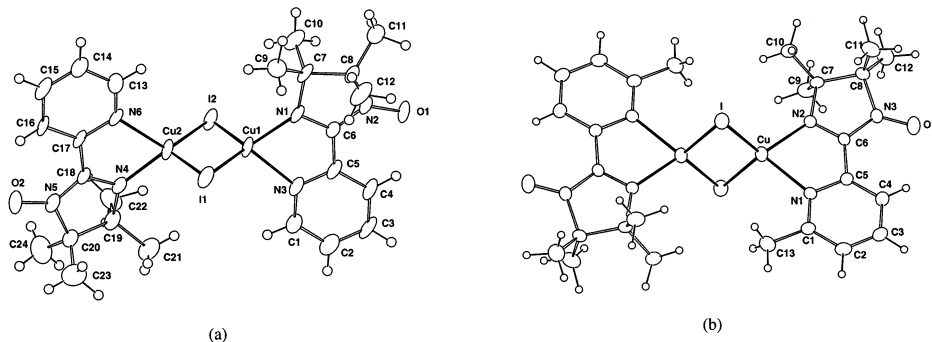


Fig. 4. The iodide bridged dinuclear structure of (a)  $[\text{Cu}(\mu\text{-I})(\text{impy})]_2$  and (b)  $[\text{Cu}(\mu\text{-I})(\text{impepy})]_2$ .

#### 4. Assemblies with Cu(I) halides

Cu(I) halocuprates have a wide variety of structures. Molecules form discrete geometries of varying nuclearity or polymeric extended systems. If organic radicals are introduced into the halocuprate cluster or network, interesting magnetic materials might be obtained. In this section, the crystal structures and magnetic properties of halogen bridged dinuclear and tetranuclear copper(I) complexes with imino nitroxide are presented [32].

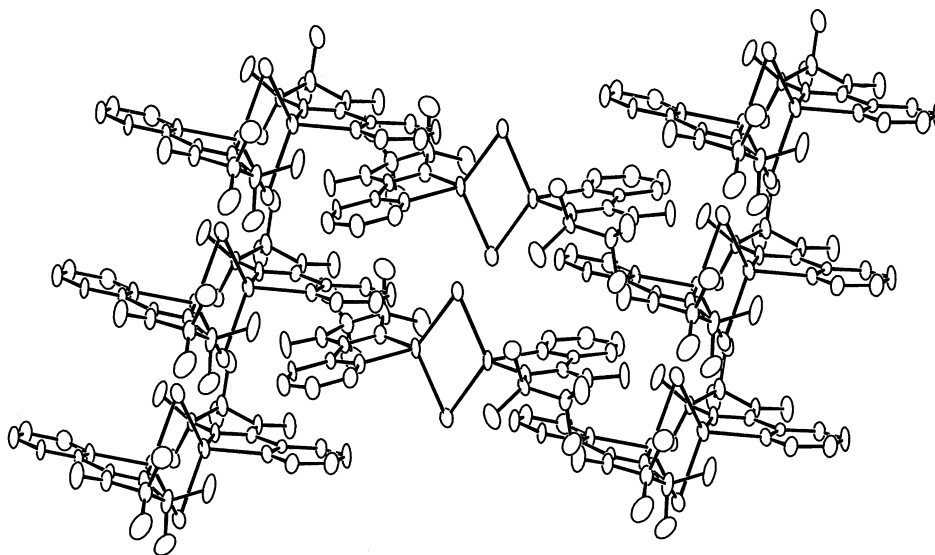


Fig. 5. The 2D structure of  $[\text{Cu}(\mu\text{-I})(\text{impy})]_2$ .

#### 4.1. Two-dimensional network of imino nitroxides in $[\text{Cu}(\mu\text{-I})(\text{impy})]_2$ and $[\text{Cu}(\mu\text{-I})(\text{immepy})]_2$

The complex molecule in  $[\text{Cu}(\mu\text{-I})(\text{impy})]_2$  (Fig. 4a) and  $[\text{Cu}(\mu\text{-I})(\text{immepy})]_2$  (Fig. 4b) consists of discrete dimers in which two copper(I) ions are separated by 2.529(2) and 2.6869(8) Å, respectively, and are bridged by two iodide ions. The coordination geometry about the Cu(I) ions is a distorted tetrahedron and four coordination sites are occupied with two nitrogen atoms and two iodide ions. The Cu–N(pyridine), Cu–N(imino nitroxide), and Cu–I distances are 2.162(9)–2.173(3), 2.005(9)–2.030(3), and 2.571(2)–2.631(2) Å, respectively.

In the crystal, coordinated imino nitroxides in adjacent molecules are stacked to form a one-dimensional chain and the chains are linked by  $\text{CuI}_2\text{Cu}$  units, that is, forming a two-dimensional network (Fig. 5). The stacking mode of the imino nitroxides are, however, subtly different, and this difference is responsible for the different magnetic behavior of the two complexes (Fig. 6).

The temperature dependence of magnetic susceptibilities for  $[\text{Cu}(\mu\text{-I})(\text{impy})]_2$  and  $[\text{Cu}(\mu\text{-I})(\text{immepy})]_2$  show quite different behavior (Fig. 7). On lowering the temperature, the  $\chi_m T$  value for  $[\text{Cu}(\mu\text{-I})(\text{impy})]_2$  increases and exhibits a maximum at 16 K ( $\chi_m T = 0.80 \text{ emu mol}^{-1} \text{ K}$ ) and then decreases, while a constant decrease of the value of  $\chi_m T$  down to 2 K is observed in the  $[\text{Cu}(\mu\text{-I})(\text{immepy})]_2$ . In  $[\text{Cu}(\mu\text{-I})(\text{impy})]_2$ , an intra-chain ferromagnetic interaction is predominant at an intermediate temperature range and then a weaker inter-chain (intra-molecular)

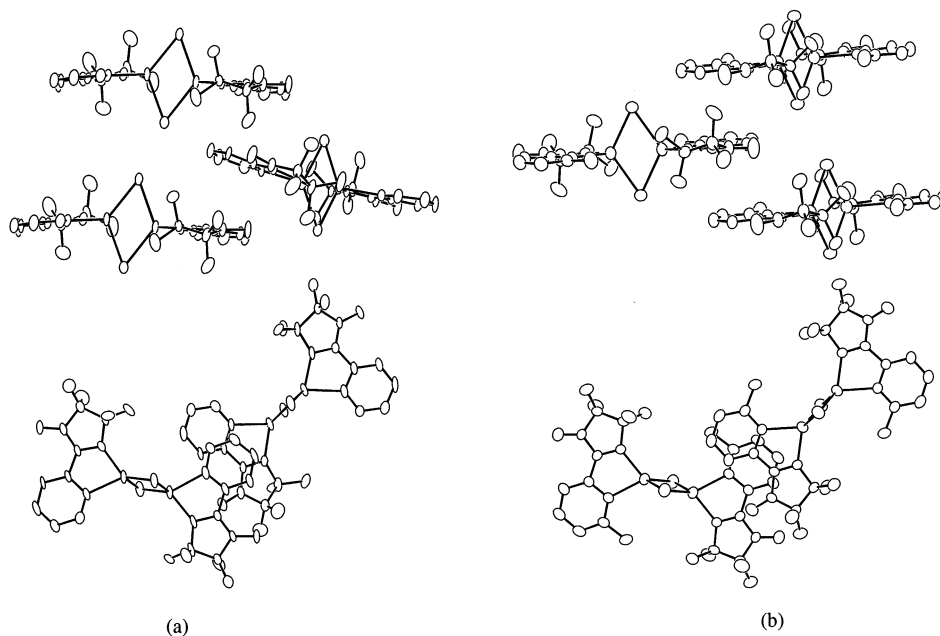


Fig. 6. Stacking diagrams of (a)  $[\text{Cu}(\mu\text{-I})(\text{impy})]_2$  and (b)  $[\text{Cu}(\mu\text{-I})(\text{immepy})]_2$ .

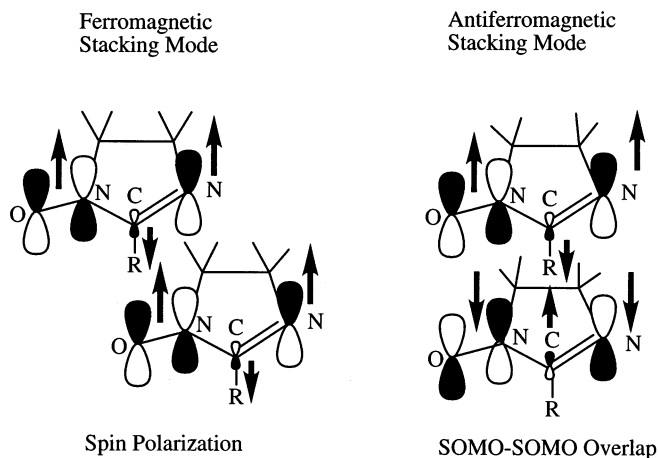


antiferromagnetic coupling is involved in the lower temperature range, while  $[\text{Cu}(\mu\text{-I})(\text{impepy})]_2$  radicals have intra- and inter-chain antiferromagnetic coupling. The magnetic data of the complexes were analyzed by isotropic Heisenberg interactions of ferromagnetic ( $J_F$ ) [33] and antiferromagnetic ( $J_{AF}$ ) [34] intrachain interactions with weak interchain (intramolecular) antiferromagnetic interactions. Least-squares calculation of the magnetic susceptibility data yielded ferromagnetic ( $J_F$ ) and antiferromagnetic ( $J_{AF}$ ) coupling constants for  $[\text{Cu}(\mu\text{-I})(\text{impy})]_2$  and  $[\text{Cu}(\mu\text{-I})(\text{impepy})]_2$  of 5.8(2) and  $-0.68(2) \text{ cm}^{-1}$ , respectively.

The sign and magnitude of the intermolecular magnetic interactions depend strongly on the relative arrangement of the stacked imino nitroxyl groups [35,36]. Two types of stacking modes are responsible for the ferromagnetic and antiferromagnetic intra-chain interactions (Scheme 3).

1. Ferromagnetic stacking mode (McConnell mechanism [37]): Spin polarization induces opposite or negative spin density on a molecule. If molecules overlap with opposite signs of the spin density, an intermolecular ferromagnetic interaction would be expected.
2. Antiferromagnetic stacking mode (SOMO–SOMO overlap): when two SOMOs overlap, bonding and antibonding orbitals are formed. Two electrons from the SOMOs locate on the bonding MO, and the singlet state will be the ground state. SOMO–SOMO overlap stabilizes the antiferromagnetic state and this situation can be regarded as a weak covalent bond.

In imino nitroxyl groups, the positive spins are populated over the N–O groups and imino nitrogen atoms, while a small negative spin density appears on the central  $\text{sp}^2$  carbon [38,39]. Structural analysis reveals that a short intermolecular contact in  $[\text{Cu}(\mu\text{-I})(\text{impy})]_2$  involves the oxygen atom of the N–O group and the  $\text{sp}^2$  carbon atom of the adjacent molecule ( $\text{O}\cdots\text{C} = 3.33(1) \text{ \AA}$ ). The corresponding intermolecular contact ( $\text{O}\cdots\text{C}$ ) in  $[\text{Cu}(\mu\text{-I})(\text{impepy})]_2$  is  $3.751(8) \text{ \AA}$ . These two atoms carry an opposite sign of the spin which alternate along the stack and this matches



Scheme 3.

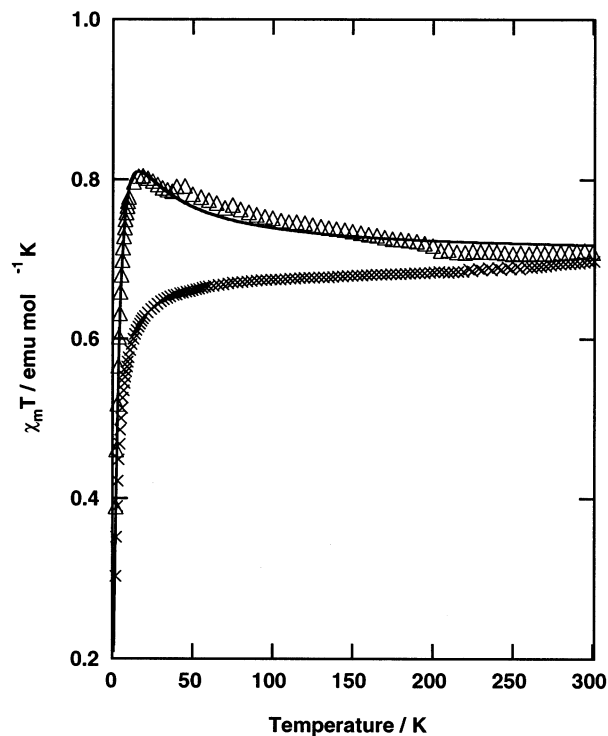


Fig. 7. Magnetic data for ( $\Delta$ )  $[\text{Cu}(\mu\text{-I})(\text{impy})]_2$  and ( $\times$ )  $[\text{Cu}(\mu\text{-I})(\text{impepy})]_2$ .

McConnell's criteria. The observed contact distances in the complexes suggest that the spin polarization leading to the intra-chain ferromagnetic interaction is more effective for  $[\text{Cu}(\mu\text{-I})(\text{impy})]_2$  than for  $[\text{Cu}(\mu\text{-I})(\text{impepy})]_2$ . On the other hand, in  $[\text{Cu}(\mu\text{-I})(\text{impepy})]_2$  the conjugated imino-nitroxyl fragments of two adjacent molecules stack with a parallel alignment ( $6.8(4)^\circ$ ), while in  $[\text{Cu}(\mu\text{-I})(\text{impy})]_2$  two imino-nitroxyl planes tilt toward each other with an angle of  $22.0(8)^\circ$  (Fig. 6). A  $\sigma$ -type overlap (SOMO–SOMO overlap) of the nitronyl nitroxide  $\pi^*$  orbital leads to the antiferromagnetic interaction and this will be maximum when the adjacent N–O groups are parallel. The resulting overlap in  $[\text{Cu}(\mu\text{-I})(\text{impepy})]_2$  favors the antiferromagnetic interaction, while the tilted stacking in  $[\text{Cu}(\mu\text{-I})(\text{impy})]_2$  diminishes the antiferromagnetic contribution. As a result, in spite of the fact that the spin polarization contributes to the stabilization of the intermolecular ferromagnetic interaction, the intrachain magnetic interaction for  $[\text{Cu}(\mu\text{-I})(\text{impy})]_2$  is ferromagnetic and that for  $[\text{Cu}(\mu\text{-I})(\text{impepy})]_2$  is antiferromagnetic.

#### 4.2. Radical cubane of $[\text{Cu}_4\text{Br}_4(\text{bisimph})_2]$

The reaction of a biradical, bisimph, with  $[\text{Cu}(\text{I})(\text{CH}_3\text{CN})_4](\text{PF}_6)$  and NaBr in methanol gave a bromo-bridged cubane type tetranuclear Cu(I) complex,

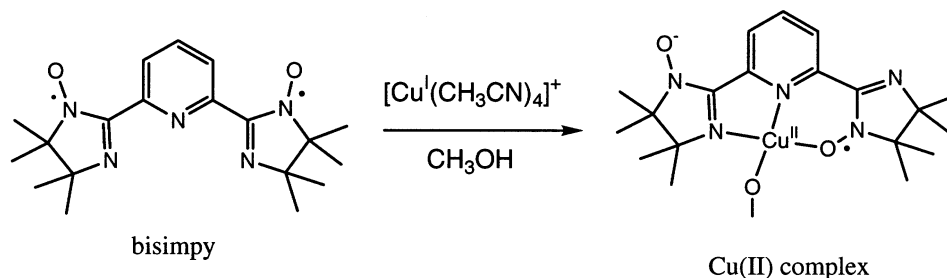
$[\text{Cu}_4\text{Br}_4(\text{bisimph})_2]$  (Fig. 8) [40]. Each Cu(I) ion in the complex has a distorted tetrahedral coordination geometry with imino nitrogen atoms (Cu–N: 1.965(5)–1.988(5) Å) and three  $\mu_3$ -Br ions (Cu–Br: 2.489(1)–2.711(1) Å). In the complex, the  $\text{Cu}_4\text{Br}_4$  core has a distorted cubane structure and the four imino nitroxides (radicals) are assembled to form a radical cubane. For this complex,  $\chi_m T$  values below 100 K showed a gradual decrease as the temperature decreased, which implies that antiferromagnetic interactions are operative, and the coupling constant  $J$  ( $H = -2J \sum S_i \cdot S_j$ ) for four imino nitroxyl radicals is estimated to be less than  $-1 \text{ cm}^{-1}$ .

## 5. Radical helix of Cu(II) imino nitroxide

The coordination geometry of the metal ions sometimes affects their redox property [41,42]. Cu(I) ions prefer a tetrahedral coordination, while Cu(II) ions tends to have square planar, square pyramidal, or trigonal bipyramidal coordination.

Reaction of  $[\text{Cu}(\text{I})(\text{CH}_3\text{CN})_4](\text{PF}_6)$  with bisimpy gave dark red crystals, which was characterized as a Cu(II) complex,  $[\text{Cu}(\text{II})(\text{imapy})](\text{PF}_6)$  (imapy: reduced form of bisimpy) [43]. During the reaction, the Cu(I) ion was oxidized to the Cu(II) ion, while the one of the imino-nitroxides of bisimpy was reduced to the imino-hydroxyamino anion (Scheme 4).

The geometrical requirement of the tridentate bisimpy ligand, which compels the Cu ion to have the square planar coordination, prompts oxidation of the Cu(I) ion.  $[\text{Cu}(\text{II})(\text{imapy})](\text{PF}_6)$  crystallizes in the non-centrosymmetric tetragonal space group  $P4_32_12$ , whose absolute structure was determined by the Flack's parameter [44]. The powder CD spectrum revealed that  $[\text{Cu}(\text{II})(\text{imapy})](\text{PF}_6)$  is a 1:1 mixture of crystals with the space group of  $P4_32_12$  and  $P4_12_12$ . The coordination geometry about the Cu(II) ion is square planar with two nitrogen and two oxygen atoms, where one of the oxygen atoms comes from the imino-hydroxyamino anion of the next molecule. The Cu(II) ions are bridged by the imino-hydroxyamino anion to form a one-dimensional structure along the  $c$ -axis, and each Cu(II) ion has a coordinated imino nitroxide. The complex molecule locates on the crystallographic



Scheme 4.

fourfold screw axis so that imino nitroxides added to the Cu(II) chain have a counter-clockwise helical arrangement in the crystalline (Fig. 9).

Analysis of the magnetic susceptibility data led to the intra-chain (Cu(II)–Cu(II) interaction) and the Cu(II)–radical interactions being  $-6(1)$  and  $-23(1) \text{ cm}^{-1}$ , respectively.

## 6. Helical assembly of imino nitroxide diradical with Ag(I) ions

In this section, double-stranded radical helicates assembled by Ag(I) ions are presented [45,46]. Radical ligands in this section are pyrd-im<sub>2</sub>, bpy-im<sub>2</sub> and bisimpy,

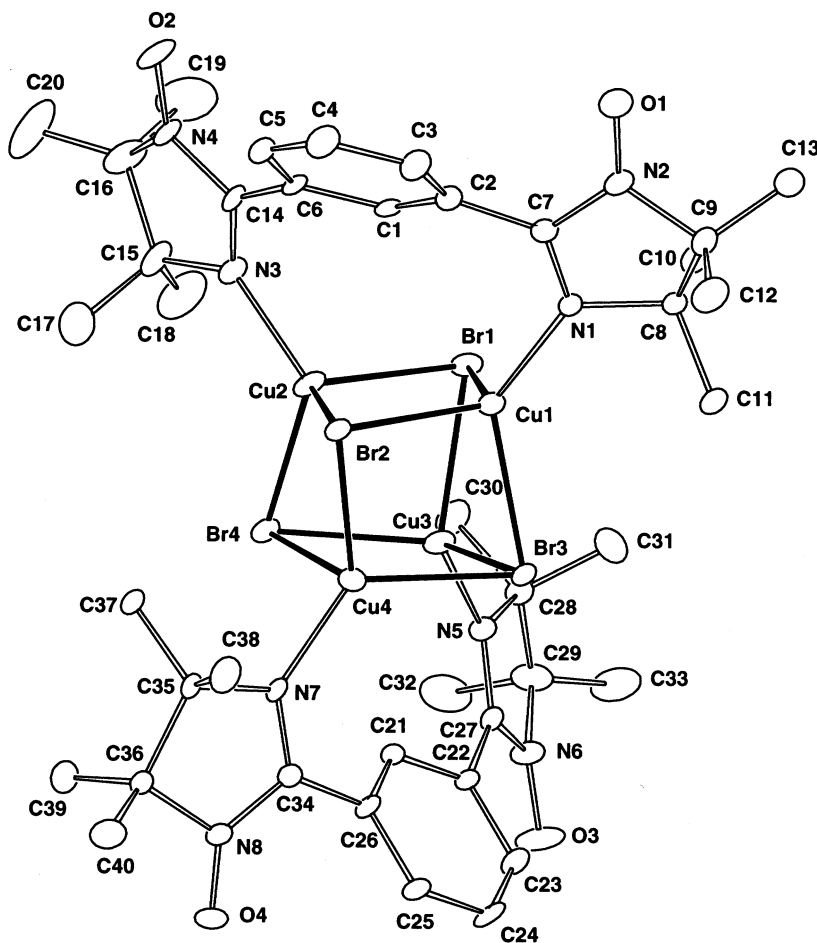


Fig. 8. The radical cubane of  $[\text{Cu}_4\text{Br}_4(\text{bisimph})_2]$ .

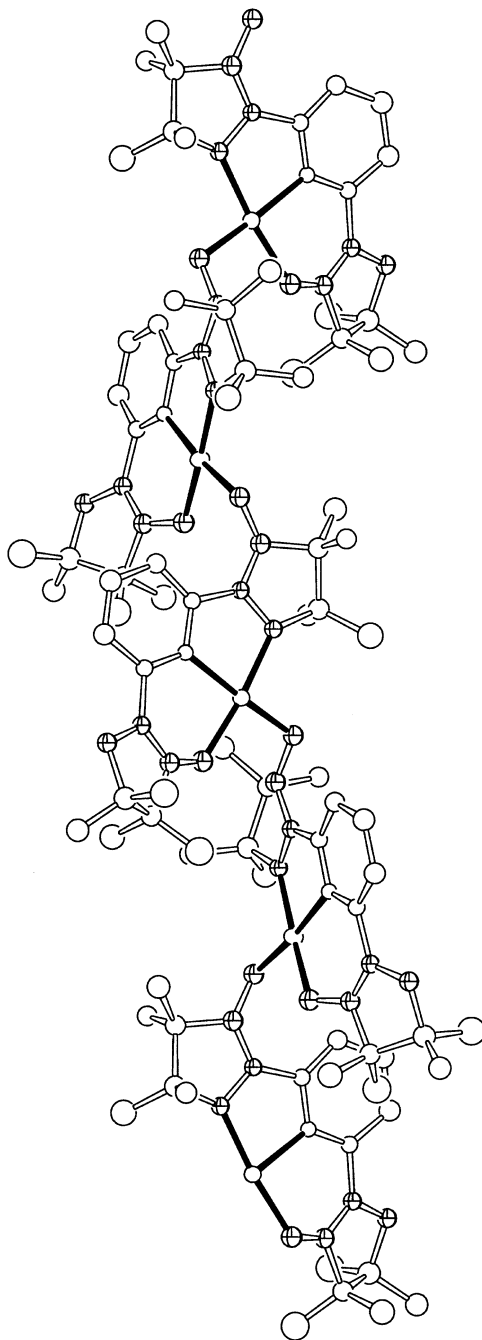


Fig. 9. The radical helix of  $[\text{Cu}(\text{II})(\text{imapy})]^+(\text{PF}_6)^-$ .

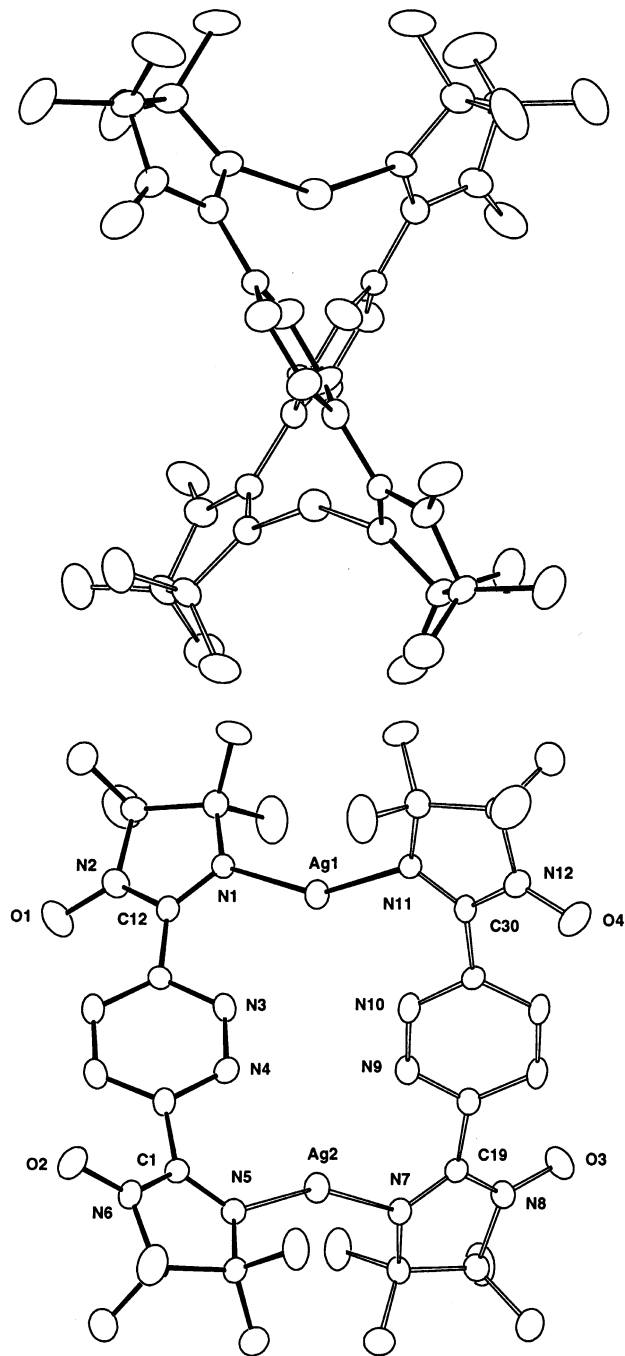


Fig. 10. The radical double helix of  $[\text{Ag}_2(\text{pyrd-im}2)_2]^+$ .

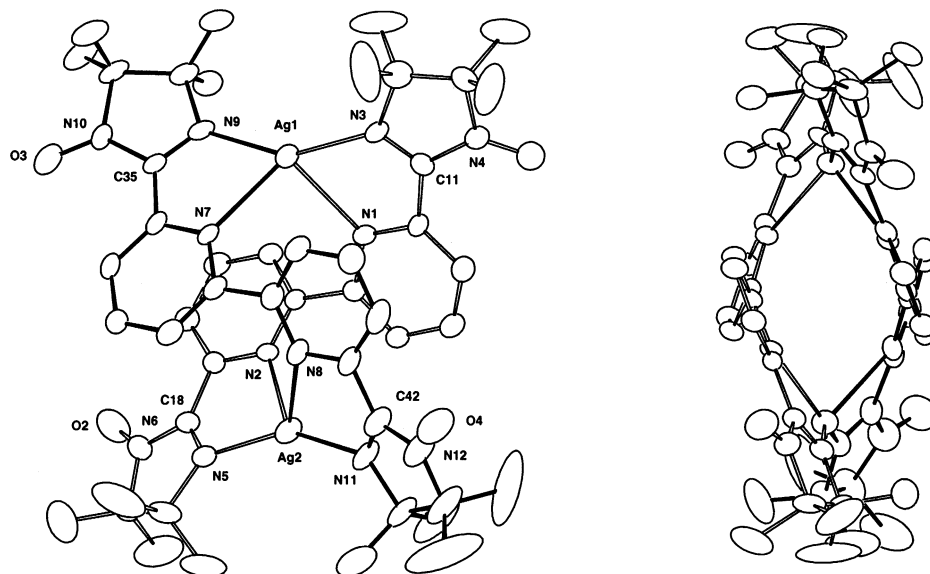


Fig. 11. The radical double helix of  $[\text{Ag}_2(\text{bpy-im}_2)_2]^+$ .

which have two imino nitroxide linked by pyridazine, bipyridine, and pyridine, respectively. Intra-ligand magnetic interactions between imino nitroxyl groups in pyrd-im<sub>2</sub> and bisimpy are supposed to have antiferromagnetic and ferromagnetic interactions, respectively, which can be understood by the spin polarization of the nitroxyl spin to the linked pyridazine and pyridine groups [47]. On the other hand, a negligibly small magnetic interaction is expected for bpy-im<sub>2</sub> because of the lack of  $\pi$  conjugation of the whole bipyridyl moiety.

Complexes  $[\text{Ag}_2(\text{pyrd-im}_2)_2](\text{PF}_6)_2 \cdot 2\text{CH}_3\text{OH}$  (Fig. 10) and  $[\text{Ag}_2(\text{bpy-im}_2)_2](\text{PF}_6)_2 \cdot \text{CH}_3\text{OH}$  (Fig. 11) have a dinuclear Ag(I) unit bridged by diradicals. Ag(I) ions either have tetrahedral four-coordination or two coordination with a bent structure, where bond lengths of Ag(I)–N(iminyl nitrogen) (2.129(4)–2.163(5) and 2.174(6)–2.230(7) Å) are short in contrast to bond distances of Ag(I)–N(pyridazyl or pyridyl group) (2.672(6)–2.750(6) or 2.477(6)–2.552(6) Å). The two Ag(I) ions are separated by 5.352(2) and 6.025(2) Å for  $[\text{Ag}_2(\text{pyrd-im}_2)_2](\text{PF}_6)_2 \cdot 2\text{CH}_3\text{OH}$  and  $[\text{Ag}_2(\text{bpy-im}_2)_2](\text{PF}_6)_2 \cdot \text{CH}_3\text{OH}$ , respectively. The structures of the complex molecules are best described as double-stranded helicates with the coordinated radical–ligands being twisted around the Ag(1)–Ag(2) axis, that is, four imino nitroxide are arranged in a helix in the complex. The angles of twist, that is, the angles of rotation of the helix, between two imino nitroxyl planes on the successive silver centers are 59 and 70° for  $[\text{Ag}_2(\text{pyrd-im}_2)_2](\text{PF}_6)_2 \cdot 2\text{CH}_3\text{OH}$  and  $[\text{Ag}_2(\text{bpy-im}_2)_2](\text{PF}_6)_2 \cdot \text{CH}_3\text{OH}$ . Thus, the full turns of the helix would involve 6.1 and 5.1 silver ions, so the helical pitches (length per turn) are about 33 and 31 Å, respectively.

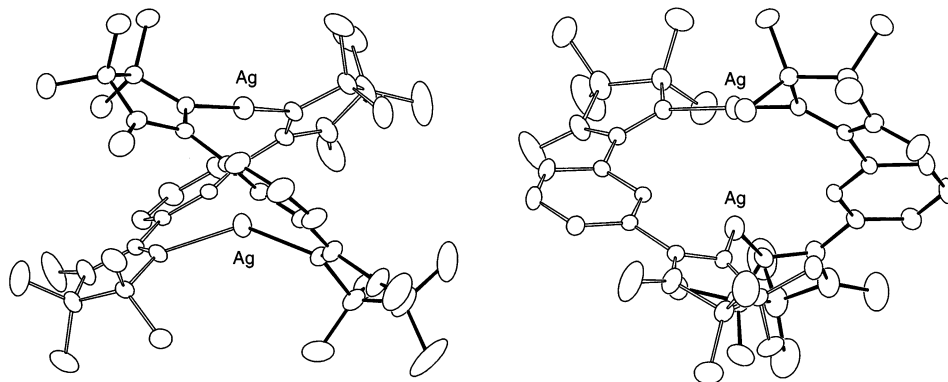


Fig. 12. The radical double helix of  $[\text{Ag}_2(\text{bisimpy})_2]^+$ .

The diradical ligand, bisimpy, has two imino nitroxyl fragments linked by a pyridyl group in the *meta*-position. Thus, the intra-ligand imino nitroxyl distances are the shortest for the diradicals presented in this paper.  $[\text{Ag}_2(\text{bisimpy})_2](\text{PF}_6)_2$  has the same double helical structure composed of two silver ions with two diradical ligands as the above two complexes (Fig. 12). Although the metal to ligand bond distances for  $[\text{Ag}_2(\text{bisimpy})_2](\text{PF}_6)_2$  are in the same range as the above mentioned Ag(I) double helical complexes, the intra-molecular Ag(I)–Ag(I) distance is 2.8942(6) Å, the number of silver ions in the full turn of the helix is 8.6, and the helical pitch is 25 Å.

Magnetic susceptibility measurements for the three silver complexes showed that intra-ligand antiferromagnetic ( $-70.8 \text{ cm}^{-1}$ ) and ferromagnetic ( $28.6 \text{ cm}^{-1}$ ) interactions are operative for  $[\text{Ag}_2(\text{pyrd-im}_2)_2](\text{PF}_6)_2 \cdot 2\text{CH}_3\text{OH}$  and  $[\text{Ag}_2(\text{bisimpy})_2](\text{PF}_6)_2$ , respectively, and magnetic interactions through the Ag(I) ions are negligibly small.

## 7. Conclusion

Combinations of organic radicals and diamagnetic Cu(I) and Ag(I) ions give a variety of molecular based assemblies, which may have very interesting structures and magnetic properties. In the assemblies, the diamagnetic metal ions act as joints and as magnetic couplers of organic radicals. More effort is justified to prepare not only radical oligomers but also pds dimensional compounds; this approach offers promising perspectives on synthesizing novel organic magnetic materials such as helical and chiral magnets.

## Acknowledgements

This work was in part supported by a Grand-in-Aid for Scientific Research from the Ministry of Education, Science, and Culture, Japan.



## References

- [1] J.-M. Lehn, *Supramolecular Chemistry*, VCH, Weinheim, 1995.
- [2] V. Balzani, *Tetrahedron* 48 (1992) 10443.
- [3] E.C. Constable, *Tetrahedron* 48 (1992) 10013.
- [4] A. Williams, *Chem. Eur. J.* 3 (1997) 15.
- [5] P.N.W. Baxter, J.-M. Lehn, J. Fischer, M.-T. Youinou, *Angew. Chem. Int. Ed. Engl.* 33 (1994) 2284.
- [6] J.-M. Lehn, A. Rigault, *Angew. Chem. Int. Ed. Engl.* 27 (1988) 1095.
- [7] R. Ziessel, A. Harriman, J. Suffert, M.-T. Youinou, A. De Cian, J. Fisher, *Angew. Chem. Int. Ed. Engl.* 36 (1997) 2509.
- [8] K.T. Potts, M. Keshavarz-K, F.S. Tham, K.A.G. Raiford, C. Arana, H.D. Abruna, *Inorg. Chem.* 32 (1993) 5477.
- [9] R.F. Carina, G. Bernardinelli, A.F. Williams, *Angew. Chem. Int. Ed. Engl.* 32 (1993) 1463.
- [10] C. Piguet, G. Bernardinelli, B. Bocquet, O. Schaad, A.F. Williams, *Inorg. Chem.* 33 (1994) 4112.
- [11] L.D. Barron, J. Vrbancich, *Mol. Phys.* 51 (1984) 715.
- [12] G.L.J.A. Rikken, E. Raupach, *Nature* 390 (1984) 493.
- [13] L. Subramanian, R. Hoffmann, *Inorg. Chem.* 31 (1993) 1021.
- [14] M. Vitale, C.K. Ryu, W.E. Palke, P.C. Ford, *Inorg. Chem.* 33 (1994) 561.
- [15] C.L. Raston, A.H. White, *J. Chem. Soc. Dalton Trans.* (1976) 2153.
- [16] S. Anderson, S. Jagner, *Acta Chem. Scand. A* 40 (1986) 177.
- [17] S. Jagner, G. Helgesson, *Adv. Inorg. Chem.* 37 (1991) 1.
- [18] G.A. Bowmaker, *Adv. Spectrosc.* 14 (1987) 1.
- [19] K.P. Bigalke, A. Hans, H. Hartl, *Z. Anorg. Allg. Chem.* 563 (1998) 96.
- [20] M. Hoyer, H. Hartl, *Z. Anorg. Allg. Chem.* 587 (1990) 23.
- [21] J.H. Osiecki, E.F. Ullman, *J. Am. Chem. Soc.* 90 (1968) 1078.
- [22] P. Chaudhuri, M. Winter, B.B.C. Della Védova, E. Bill, A. Trautwein, S. Gehring, P. Fleischhauer, B. Nuber, J. Weis, *Inorg. Chem.* 30 (1991) 2148.
- [23] P. Chaudhuri, M. Winter, P. Fleischhauer, W. Haase, U. Flörke, H.J. Haupt, *J. Chem. Soc. Chem. Comm.* (1990) 1728.
- [24] G.A. Fox, C.G. Pierpont, *Inorg. Chem.* 31 (1992) 3718.
- [25] G.A. Abakumov, V.K. Cherkasov, M.P. Bubnov, O.G. Ellert, U.V. Rakitin, L.N. Zakharov, Y.T. Struchkov, U.N. Saf'yanov, *Isv. Akad. Nauk. SSSR*, (1992) 2315.
- [26] C.W. Lange, B.J. Conklin, C.G. Pierpont, *Inorg. Chem.* 33 (1994) 1276.
- [27] D.M. Adams, A.L. Rheingold, A. Dei, D.N. Hendrickson, *Angew. Chem. Int. Ed. Engl.* 32 (1993) 391.
- [28] A. Ozarowski, B.R. McGarvey, A. El-Hadad, Z. Tian, D.G. Tuck, D.J. Krovich, G.C. DeFtis, *Inorg. Chem.* 32 (1993) 841.
- [29] S. Bruni, A. Caneschi, F. Cariati, C. Delfs, A. Dei, D. Gatteschi, *J. Am. Chem. Soc.* 116 (1994) 1388.
- [30] H. Oshio, T. Watanabe, A. Ohto, A.T. Ito, U. Nagashima, *Angew. Chem. Int. Ed. Engl.* 33 (1994) 670.
- [31] H. Oshio, T. Watanabe, A. Ohto, A.T. Ito, T. Ikoma, S. Tero-Kubota, *Inorg. Chem.* 36 (1997) 3014.
- [32] H. Oshio, T. Watanabe, A. Ohto, T. Ito, H. Masuda, *Inorg. Chem.* 35 (1996) 472.
- [33] G.A. Baker, G.S. Rushbrooke, H.E. Gilbert, *Phys. Rev.* 135 (1964) A1272.
- [34] J.C. Bonner, M.E. Fisher, *Phys. Rev.* 1964 (1964) A640.
- [35] A. Caneschi, F. Ferrara, D. Gatteschi, P. Rey, R. Sessoli, *Inorg. Chem.* 29 (1990) 1756.
- [36] F.L. Panthou, D. Luneau, J. Laugier, P. Rey, *J. Am. Chem. Soc.* 115 (1993) 9095.
- [37] H.M.J. McConnel, *Chem. Phys.* 39 (1963) 1910.
- [38] A. Zheludev, V. Barone, M. Bonnet, B. Delley, A. Grand, E. Ressouche, P. Rey, R. Subra, J. Schweizer, *J. Am. Chem. Soc.* 116 (1994) 2019.
- [39] K. Yamaguchi, M. Okumura, M. Nakano, *Chem. Phys. Lett.* 191 (1992) 237.

- [40] Crystal data for  $[\text{Cu}_4\text{Br}_4(\text{bisimp})_2]$ : triclinic space group  $P\bar{1}$ ,  $a = 13.774(3)$ ,  $b = 15.743(3)$ ,  $c = 12.762 \text{ \AA}$ ,  $\alpha = 91.85(2)$ ,  $\beta = 97.85(2)$ ,  $\gamma = 65.17(2)^\circ$ ,  $V = 2487.0(9) \text{ \AA}^3$ ,  $Z = 2$ ,  $R = 0.044$ , and  $R_w = 0.059$ .
- [41] H. Oshio, K. Toriumi, Y. Hayashi, J. Chem. Soc. Dalton Trans. (1990) 293.
- [42] A. Livoreil, C.O. Dietrich-Buchecker, J.-P. Sauvage, J. Am. Chem. Soc. 116 (1994) 9399.
- [43] H. Oshio, T. Watanabe, A. Ohto, T. Ito, Inorg. Chem. 36 (1997) 1608.
- [44] H.D. Flack, Acta Crystallogr., Sect. A 39 (1994) 876.
- [45] H. Oshio, T. Yaginuma, T. Ito, Inorg. Chem. 38 (1999) 2750.
- [46] H. Oshio, M. Yamamoto, T. Ito, J. Chem. Soc. Dalton Trans. (1999) 2641.
- [47] H.M. McConnell, J. Chem. Phys. 39 (1963) 1910.